CONF-830103--2

LA-UR -82-1800

Los Alamos National Laboratory is operated by the University of California for the United States Department of Energy under contract W-7405-ENG-36

LA-UR--82-1800

DE82 017329

TITLE: FAILURE MODES OF A CONCRETE NUCLEAR-CONTAINMENT BUILDING SUBJECTED TO HYDROGEN DETONATION

AUTHOR(S): L. Erik Fugelso
T. A. Butler

SUBMITTED TO: SECOND INTERNATIONAL TOPICAL MEETING ON NUCLEAR THERMALHYDRAULICS
SANTA BARBARA, CA, JANUARY 11-14, 1983

Los Alamos National Laboratory
Los Alamos, New Mexico 87545

FAILURE MODES OF A CONCRETE NUCLEAR CONTAINMENT BUILDING SUBJECTED TO HYDROGEN DETONATION

L. Erik Fugelso
T. A. Butler

Los Alamos National Laboratory
Los Alamos, New Mexico 87545

ABSTRACT

Calculated response for the Indian Point reactor containment building to static internal pressure and one case of a dynamic pressure representing hydrogen combustion and detonation are presented. Comparison of the potential failure modes is made.

INTRODUCTION

During a postulated severe accident in a pressurized water reactor (PWR) loss of both natural convection cooling and the emergency cooling system could lead to reactor core dryout, heat up, and eventual meltdown. This will subsequently lead to generation of steam and noncondensible gases that could conceivably raise the internal pressure of the PWR containment building enough to cause it to fail. Also, during the accident scenario the core cladding oxidizes producing hydrogen that can either burn or detonate causing transient loads to act on portions of the containment. Because the containment building is the last line of defense in protecting the public from a release of fission products, the ultimate pressure capacity of the building becomes an important input to analysis of the consequences of core-melt accidents. We address the question of ultimate containment capability under quasistatic overpressurization and containment response to hydrogen detonation for the Indian Point nuclear reactor.

A previous study performed by Sandia National Laboratories (SNL) on Indian Point[1] concluded that the failure mode for the building was excessive hoop strain in the cylindrical sidewall. Independent analyses performed by the utilities were in good agreement with the conclusions drawn.[2] Because of the time frame involved, these initial studies left out considerable detail

and used several simplifying assumptions. The study used design material properties. In the current work we developed a more detailed models of the building and used as-built material properties for the critical structural components.

For evaluating the response to quasistatic overpressurization we used two-dimensional axisymmetric finite element models. To determine response of containment buildings to postulated hydrogen detonations, we subjected the Indian Point containment building to a simplified transient load developed to simulate detonation of hydrogen in its hemispherical dome.

The specific building modeled was the Indian Point Unit No. 3 containment. Applied loads from internal pressure, weight of structure and equipment were included, but we do not include response to loads induced from thermal gradients.

In the following section, the hydrogen-air mixture detonation and deflagration properties pertinent to the analysis are summarized. Then, the description of the Indian Point containment structure and the structural modelling associated with the finite element calculation are detailed. Comparison of this model with the static internal pressurization test establishes to the validity of the modeling. Static and dynamic response to the structural loads representative of a typical combustion and detonation are presented in the following sections.

HYDROGEN DETONATION AND COMBUSTION CHARACTERISTICS

During the course of a severe nuclear reactor accident hydrogen can be generated by steam reacting with cladding material in the reactor core. Figure 1, which is based on experimental information from Refs. 3 and 4, gives detonation pressure as a function of hydrogen concentration. Also shown on the figure are the ignition and detonation limits and the theoretical pressures generated by hydrogen burns and detonations. When the hydrogen concentration reaches the lower flammability limit of $\sim$ 5 vol% at room temperature and 1 atm pressure, it can be ignited and generate a slowly rising (on the order of several seconds) pressure. Mark[5] notes that the 28 psi-(0.19 MPa)-pressure spike in the TMI-2 containment was attributed to the burning of a uniform hydrogen-air mixture having a hydrogen concentration of about 8.5 vol%. If the hydrogen concentration exceeds 19% it will detonate rather than burn.[3,4] Because of the maximum amount of available hydrogen,

these concentrations could occur only if the hydrogen is confined to a small compartment within the structure of if it becomes stratified in a larger volume. Stratification is unlikely because the hydrogen is introduced near the bottom of the containment and will tend to rise. As it rises through the containment its diffusion characteristics in air along with natural convection currents generated within the containment will tend to keep it mixed. For this study we assume that stratification does occur and a detonable mixture of hydrogen fills the hemispherical dome of the Indian Point containment building. A concentration of 25% H is assumed in order to generate the maximum pressure possible.

Because the rise in pressure that occurs as the mixture burns generates dynamic loads that have long characteristic periods when compared to the vibrational frequencies of the structure, the building will respond in a quasistatic manner and potential damage can be predicted based on conclusions of a static analysis.

The dynamics of hydrogen combustion in a closed container has been theoretically and experimentally determined. [4] The form of the pressure-time history at the wall of a rigid spherical container ignited at the center is a t^3 rise to the maximum pressure followed by the constant pressure.

For a detonation wave emanating from a point the detonation velocity and pressure are constant. For a 25% concentration of hydrogen at 1 atm initial pressure the velocity is 1850 m/s (6070 ft/s) and the pressure, P_D, is 14 atm[6]. If the detonation wave strikes a rigid wall normal to its surface the peak reflected pressure acting on the wall is 2.56 P_D. When a detonation wave strikes a rigid wall at an oblique angle the peak reflected shock strength is a function of the angle of incidence. The reflected pressure is not substantially modified until the angle of incidence exceeds 45^0. Between 45^0 and 90^0 the reflected pressure drops off linearly with the angle until it is equal to the incident pressure at 90^0. The reflected pressure history for the first pulse at the surface of a rigid spherical cavity has the form[7]

$$\frac{p}{p_D} = 0.39 + 1.00 \exp\left(-\frac{\tau}{0.28}\right) + 1.17 \exp\left(-\frac{\tau}{0.06}\right) \qquad (1)$$

where $\tau = D(T - t_a)/\lambda$

D = the detonation velocity

λ = radius of the cavity

t_a = λ/D, the time of arrival of the detonation velocity at the cavity wall.

CONTAINMENT BUILDING DESIGN

The Indian Point containment building is a reinforced concrete right vertical cylinder with a hemispherical dome and has the basic dimensions shown in Fig. 2. The only location in the structure where significant shear and moment loads develop during quasistatic pressurization is at the intersection of the cylindrical side wall with the basemat. Details of the steel reinforcing in this region are shown in Fig. 3. The details are specific for the Indian Point Unit No. 3 containment. However, except for the location of the seismic reinforcement, Unit No. 2 has the same steel placement. The three vertical reinforcing patterns shown in the figure are alternately repeated around the building.

The steel liner for the Indian Point building is constructed of ASTM A442 Grade 60 carbon steel. Its thickness is 6.4 mm (0.25 in.) on the containment floor and 12.7 mm (0.50 in.) on the lower portion of the cylindrical sidewall. On the upper portion of the cylindrical sidewall and inside hemispherical dome it is 9.5 mm(0.38 in.) thick. At penetrations the liner is reinforced to 19.0 mm (0.75 in.). In the cylindrical portion of the containment liner anchors are a grid of 12.7 mm(0.5 in.)-diam bent welding studs. In the dome a grid of T-bars is used along with the bent welding studs.

The building has over 100 penetrations for electrical and mechanical access. Two large openings are provided for personnel and equipment access into the containment structure. The largest penetration is the equipment hatch with a diameter of 15.5 m (18 ft). The personnel lock has an opening size of 2.6 m(8.5 ft) diam. Steel reinforcement in the concrete is continuous but bent at the larger penetrations. The equipment hatch and personnel lock have additional reinforcement to insure that these penetrations do not constitute weak points in the structure.

STRUCTURAL MODELING

The Indian Point containment building is, basically, an axisymmetric structure so a two-dimensional axisymmetric finite element model was used to determine its failure mode and associated failure pressure. Several features of the structure are not axisymmetric and therefore had to either be approximated in the two-dimensional model, neglected, or analyzed separately. All of the penetrations, except for the two large access hatches, are small compared to basic structural dimensions (for example, the diameters are less than wall thickness) . This is especially true because they are not in high moment or shear areas and the membrane carrying reinforcement is continuous at their locations and can therefore be neglected.

The hoop-oriented steel reinforcement bars are the only ones that are truly axisymmetric. However, a close approximation of the effect of radially- and meridionally-oriented steel can be obtained by smearing its effect and including it as discrete truss elements in the model. The building includes structural steel for seismic reinforcement that is not oriented along any of the three principal directions (hoop, radial, or meridional). The effect of this structural steel was included by projecting its area to the hoop and meridional directions. The weight distribution affects the gravity loads on the base slab and, therefore the uplift experienced when the structure is pressurized. Even with the above assumptions, the resulting two-dimensional models are accurate representations of the structures, especially in the areas where failure is predicted to occur.

The ADINA finite element code[8] was used to develop the two-dimensional finite element model. It has been successfully applied to other reactor structures.[9] It includes a good concrete constitutive model and the Los Alamos version of the code has a nonlinear, two-dimensional shell finite element for simulating the containment liners. The two-dimensional mesh generated for representing the building is shown in Fig. 4. Mesh density was chosen to give good resolution of stresses in high moment and shear areas and to place nodal points to which the liner is attached at the approximate actual liner anchor spacing.

Boundary conditions on the models include those enforcing axisymmetric motion on the axis of symmetry. Under the base slab we have included nonlinear springs to simulate the restraining effect of the ground on downward motion. These springs are very stiff in compression and have no stiffness in

tension. This allows the building's base slab to uplift with no exterior restraint. We neglect the effect of soil around the outside of the lower portion of the cylindrical sidewall.

The concrete material model used is the tensile-cracking, compression-crushing, strain-softening model described in Ref. 10. The tensile cracking mechanism is implemented by examining the maximum principal stress at each element integration point. If this stress exceeds the uniaxial cutoff tensile stress, a failure plane (interpreted here as a "cracked" plane) has formed normal to the maximum principal stress direction. The normal stiffness across this plane is decreased to a user-specified factor times the original stiffness. The shear stiffness at this integration point is similarly reduced. We used the 8-node isoparametric axisymmetric element with a 3 by 3 array of integration points. A normal stiffness reduction factor of 0.0001 and a shear stiffness reduction factor of 0.5 was used. Table I gives the concrete material properties for the Indian Point building. They are based on a design value of 27.6 MPa (4000 psi) compressive strength.

Steel reinforcement for the building has a nominal yield strength of 60 000 psi (414 MPa). As-built material properties are presented in Tables I and II. All hoop reinforcement is represented with ring finite elements.

TABLE I

DESIGN CONCRETE MATERIAL PROPERTIES FOR THE INDIAN POINT CONTAINMENT BUILDING

Target modulus of elasticity at zero strain.	25.5 GPa (3.7 x 10^6psi)
Poisson's ratio.	0.19
Uniaxial cutoff tensile stress	2.8 MPa (400 psi)
Uniaxial maximum compressive stress.	27.6 MPa (4000 psi)
Corresponding uniaxial compressive strain.	0.002
Uniaxial ultimate compressive stress	20.0 MPa (2900 psi)
Corresponding ultimate compressive strain.	0.003

The steel liner plates were modeled with a three-node axisymmetric shell element. For the steel components, reinforcement, and liners, we used a value for Young's modulus in the elastic region of 200 GPa (29 x 10^6 psi).

TABLE II

AS-BUILT STEEL REINFORCEMENT MATERIAL PROPERTIES FOR
INDIAN POINT CONTAINMENT BUILDING

Component	Specified Yield Strength	Mean Yield Strength	Standard Deviation	% Elongation (Mean)	Standard Deviation
11	0.41 GPa (60 000 psi)	0.48 GPa (69 700 psi)	26.9 MPa (3900 psi)	19.2	2.5%
18	0.41 GPa (60 000 psi)	0.44 GPa (71 000 psi)	35.2 MPa (5100 psi)	7.4	2.3%
Steel liner	0.22 GPa (32 000 psi)	0.33 GPa (48 400 psi)	15.9 MPa (2300 psi)	26.2	1.9%

I.

COMPARISON WITH STRUCTURAL INTEGRITY TESTS

The two-dimensional analytical model of the containment building was loaded with appropriate internal pressures to compare their predicted displacements and concrete crack patterns witn those measured during the Structural Integrity Tests (SIT). The building was slowly pressurized to 0.37 MPa (54 psig) internal pressure, which is 115% of the design pressure. Pressurization was held constant at selected internal pressures to enable mapping of crack patterns. Detailed comparison of the test data and the finite element calculation is reported and summarized in Refs. 11 and 12. Comparison was good for deflections and growth of crack patterns.

CONTAINMENT STATIC RESPONSE AND FAILURE

The containment building experiences considerable concrete cracking at SIT pressures. As the internal pressure increases concrete cracking becomes more widespread, especially at the intersection of the cylindrical sidewall and basemat, which is the predicted failure point. At 0.37 MPA (54 psig) internal pressure the base of the cylindrical wall is cracked in the meridional direction from combined tensile and shear forces. Additional cracks perpendicular to these begin appearing at the base of the sidewall on the inside surface at 0.48 MPa (70 psig). When this occurs, the concrete begins losing its capability to carry shear. At 0.81 MPa (118 psig) internal pressure the shear

failure in the concrete has progressed 75% of the way through the wall. In addition, concrete on the outside of the wall has begun to crush from the high compressive loads. Any additional pressure results in additional crushing and failure to numerically converge.

As concrete cracking progresses through the wall and it is able to carry less shear, the stress in this reinforcement increases more rapidly with pressure. A partially offsetting effect is that, as the concrete cracks and crushes at this location, the moment at the intersection is reduced. Then the shear carried at the lower end of the wall is decreased somewhat. At 0.76 MPa (110 psig) internal pressure the concrete begins crushing in the outside of the wall. At 0.81 MPa (118 psig) internal pressure the stress in the shear reinforcement has reached 90% of its yield stress. Linear extrapolation of this curve indicates shear reinforcement yielding at 0.83 MPa (120 psig) internal pressure.

If the concrete carries no shear and the maximum shear force possible is developed at this intersection, simple handbook calculations show that the shear reinforcement would yield at $\sim$ 0.77 MPa (112 psig) internal pressure. If a perfect hinge develops, the shear reinforcement will not yield until the internal pressure reaches 1.54 MPa (224 psig). These are the two bounding values for this failure mode. In reality, the moment is necessarily finite until the shear reinforcement fails because it is a major contributor to the moment. Because of the highly complex and nonlinear nature of the structural behavior at this joint, we are constrained to rely on the predictions of the analytical model. It predicts failure at 0.81 MPa (118 psig) internal pressure from excess concrete cracking and crushing coupled with a loss of shear-carrying capability at the base of the cylindrical wall.

The displaced shape of the building just prior to failure is shown in Fig. 5. The displacements have been amplified by a factor of 50 to make the shape easier to visualize. The shape indicates that, even through the concrete is severely crushed and cracked at the base of the cylindrical wall, a large moment still exists.

Vertical displacements of the dome apex and outer edge of the basemat are shown in Fig. 6. The data indicate increasing flexibility of the structure in the vertical direction as concrete cracking progresses to involve more of the structure. The radial displacements shown in Fig. 7 show constant structural stiffness in the hoop direction before and after complete hoop cracking occurs between 0.21 and 0.27 MPa (30 and 40 psig) internal pressure.

Strain in the meridional reinforcement on the inside of the cylindrical sidewall at its intersection with the basemat indicates yield at ∿ 0.72 MPa (105 psig) internal pressure. The liner yields at 0.66 MPa (96 psig) internal pressure. However, its strain increases much more rapidly after 0.72 MPa when the inner reinforcement yields. At 0.81 MPa (118 psig) internal pressure the strain in the liner in the hoop direction in the cylindrical wall is approximately 0.21%, which indicates yield but not failure.

CONTAINMENT DYNAMIC RESPONSE AND FAILURE

In this section we address the capability of the containment to withstand the dynamic loads generated by hydrogen detonation. The hydrogen concentration was assumed to 25%, which will give the maximum detonation pressure. A previous study[13] assumed that this mixture completely filled the entire containment structure. This amount of hydrogen was excessive and we therefore postulated that the detonable gas concentrated in the hemispherical dome.

For the particular case studied we applied a pressure history based on Eq. 1 simultaneously to the total inside surface of the hemispherical dome. This load distribution is based on the assumption that the ignition point is at the centerline of the building at the base of the dome. Pressure was also applied simultaneously to the inside of the cylindrical sidewall between the hemispherical dome and the operating floor. The amplitude of the sidewall pressure was adjusted to account for decay of a shock passing through air. A simplifying approximation was made that the time of arrival of the pressure load is the same for all points in the structure.

The applied pressure in the dome consists of two components. For this particular case an overpressure of 0.45 MPa (65 psig) and an additional impulse of ∿ 4895 Pa-s (0.71 psi-s) act on the structure. In reality, because the complete containment volume is not filled with the detonable mixture (the dome comprises less than 25% of total containment volume), this overpressure will rapidly reduce to a fraction of its predicted value.

In Ref. 4 a bounding impulse delivered to the containment wall is reported to be 786 Pa-s (0.114 psi-s). This is less than one-sixth of the impulse we calculate based on Eq. 1. The difference in the values for the impulse apparently come from the way the burnt gas composition behind the detonation is calculated. For our model the composition is frozen and no heat conduction is allowed. The model in Ref. 6 is more complex, and therefore less conservative, allowing for heat conduction and continuing chemical reactions behind

the detonation front causing a faster reduction in pressure. As will be described below, the contribution of the impulsive component of the detonation pressure is quite low, even when our higher value is used.

Figure 8 shows the displacement response of the building to these loads at 30 ms after the shock from the detonation reaches the wall. The displacements have been amplified by a factor of 50. This particular time is 6 ms after the dome apex reaches its peak vertical displacement and 3 ms before the base of the dome reaches its peak radial displacement (Fig. 9). Even though we cannot directly compare this solution with the static solution of the preceeding section because the pressure distribution is different, a qualitative comparison gives some interesting results. The peak radial displacement at the base of the dome is $\sim$ 1.11 times the estimated static displacement if we extrapolate the static calculation to 0.90 MPa (130 psi) internal pressure. This means that the dynamic response is governed principally by the step overpressure of 0.45 MPa (65 psig) and the 4895 Pa-s (0.71 psi-s) impulse adds only 5-10% to the response. This conclusion is based on the fact that the displacement response of a linear undamped single-degree-of-freedom system to a step load is double the response if the load were applied very slowly.

The response of the building to these loads is accompanied by significant cracking of the concrete and limited plasticity in the steel reinforcement. Maximum plastic strain in the steel is 0.68% near the dome apex with most of it remaining under 0.40%. The liner response is characterized by a maximum hoop strain of 0.32% accompanied by a meridional strain of 0.19% near the dome apex at 24 ms.

Because of the many locations that a postulated detonation of a hydrogen-air mixture could occur within a containment and the different structural characteristics (for example, rectangular compartments vs the containment dome), we developed a simplified model to aid in generalizing our conclusions. The model used is a single-degree-of-freedom representation with an elastic perfectly-plastic constitutive model. Provision was made for adding the effects of viscous damping.

The equations of motion were appropriately nondimensionalized with the forcing quantity being represented by the ratio of the applied detonation pressure, P_D, to the static yield pressure, P_y. The transient nature of the applied load is represented by Eq. 1 with λ = 20.5 m (810 in.). The system frequency was set at 8 Hz, which is the approximate fundamental frequency for the Indian Point containment building.

Response was calculated for 0%, 5%, and 10% viscous damping. Results of the analysis defined the required excess ductility, μ, $\mu = \varepsilon/\varepsilon_y - 1$, of the structures to withstand specified detonation pressures. Several conclusions were drawn based on the analysis. Just as the finite element analysis previously described indicated, the response to the step overpressure portion of the load dominates the total response. Response to the impulse adds only about 10%. If we use liner strain as the measure for response in our finite element analysis, $\mu = 0.0032/0.0017 - 1.0 = 0.88$. From the simple analysis we would expect $P_D/P_y = 1.6$. Based on extrapolations of stresses in the dome area made from our previously described static analysis, $P_D/P_y = 191/136 = 1.4$. This is considered good agreement considering that the static load distribution used in calculating P_y is somewhat different than the distribution used for the dynamic calculation of building response to hydrogen detonation.

Another aspect of dynamic response that should not be neglected is the transmission of a shock through the concrete from the applied impulse. When this shock reaches the outer surface of the concrete it is reflected and the concrete experiences tensile loads that could cause spalling. If this occurs the spalling will be limited to the concrete outside of the external layer of reinforcement in the wall. Spall threshold for blast waves loading walls is given in Ref. 14. Using the appropriate numerical values for this problem, we predict no spalling unless the concrete tensile strength is less than 0.69 MPa (100 psi).

CONCLUSIONS

Dynamic calculations of the deflections of the Indian Point containment structure to one of many possible detonable H_2 air mixtures were accomplished using the finite element code ADINA with a reasonably detailed model of the concrete and the reinforcement. The hydrogen mixture was assumed to be confined to the upper hemispherical region with ignition at the center of the hemisphere and an analytical approximation was used to account for the loads. This model thus ignored complex detonation-shock interactions[13] but gives a reasonable estimate for most of the loading history. Results of our quasistatic analysis indicate the Indian Point containment building will fail at the base of its cylindrical sidewall at an internal pressure of 0.81 MPA (118 psig).

Comparison of these static failure pressures with the combustion pressures generated by the deflagration of an 8.5% hydrogen air mixture indicate that some cracking and plastic deformation would take place, but that the structure would not fail.

The analysis should be conservative because we used the hypothetical hydrogen concentration yielding maximum detonation pressures. It is unlikely that hydrogen in a reactor accident environment could even reach this concentration before igniting and burning, which would yield pressure histories that would cause response in the quasistatic mode.

REFERENCES:

1. "Report on the Zion/Indian Point Study, Vol. 1, "Sandia National Laboratories report SAND 80-0167, NUREG/CR-1410 (1980).

2. "Report on Consolidated Edison's Indian Point Unit No. 3 Containment Vessel Structural Integrity Test," for WEDCO Corporation (prepared by United Engineers and Constructors Inc.) (February, 1975).

3. M. Hertzberg, "Flamability Limits and Pressures Development in H_2-Air Mixtures," Bureau of Mines Pittsburg Research Center report 4305 (January 1981).

4. B. Lewis and G. von Elbe, Combustion, Flames and Explosions of Gases (Academic Press, New York, 1961).

5. J. C. Mark, "Notes on Hydrogen Burn with Ignitors," NRC Memorandum (December, 1981).

6. R. J. Klima and L. E. Fugelso, "1500 psi Dynamic Load Simulator," Second Conference on Military Applications of Blast Simulators" (1970).

7. F. E. Ostrem asnd L. E. Fugelso, "Feasibility of Underground Gas Detonations," DASA 1919 Final Report, Contract DA-49-146-XZ540, Defense Atomic Support AGency (1967).

8. K. J. Bathe, "ADINA: A Finite Element Program for Automatic Dynamic Incremental Nonlinear Analysis," Massachusetts Institute of Technology report 82448 (September 1975, Revised December 1978).

9. T. A. Butler and J. G. Bennett, "Nonlinear Response of a Post-Tensioned Concrete Structure to Static and Dynamic Internal Pressure Loads," Computer and Structures 13, pp. 647-659 (1981).

10. K. J. Bathe and S. Ramaswamy, "On Three-Dimensional Nonlinear Analysis of Concrete Structures," Nuc. Eng. and Design 52, 385-409 (1979).

11. T. A. Butler and L. E. Fugelso "Response of the Zion and Indian Point Containment Buildings to Severe Accident Pressures" NUREG/CR-2569 Los Alamos National Laboratory report LA-9301-MS (1982).

12. T. A. Butler, "Predications of Failure Modes for Concrete Nuclear Containment Buildings," ASME/ANS Nuclear Engineering Conference (1982).

13. R. K. Byers, "CSQ Calculations of H_2 Detonations in Zion and Sequoya," Proceedings of the Workshop on the Impact of Hydrogen in Water Reactor Safety" Vol. IV, 345-364, NUREG/CR-2017, Sandia National Laboratory SAND 81-0661 (1980).

14. W. E. Baker, P. S. Westine, J. J. Kulesy, J. S. Wilbeck, and P. A. Cox, "A Manual for the Prediction of Blast and Fragment Loadings on Structures," U.S. Department of Energy report DOE/TIC-11268, Chap. 4, pp. 149-155 (November 1980).

FIGURE CAPTIONS
"FAILURE MODES OF A CONCRETE..."

Fig. 1. Pressures produced during hydrogen burns and detonations.

Fig. 2. Indian Point containment building.

Fig. 3. Details of Indian Point cylinder--base slab intersection.

Fig. 4. Finite element mesh of Indian Point containment building.

Fig. 5. Displaced shape of Indian Point containment building just prior to failure (displacements are amplified by a factor of 50).

Fig. 6. Vertical displacements of Indian Point containment building during pressurization.

Fig. 7. Radial displacements of Indian Point containment building during pressurization.

Fig. 8. Displacement response at 6 ms of building to detonation (displacements are amplified by a factor of 50).

Fig. 9. Outward displacement versus time at the apex and the hemisphere-cylinder intersection.

Fig. 1

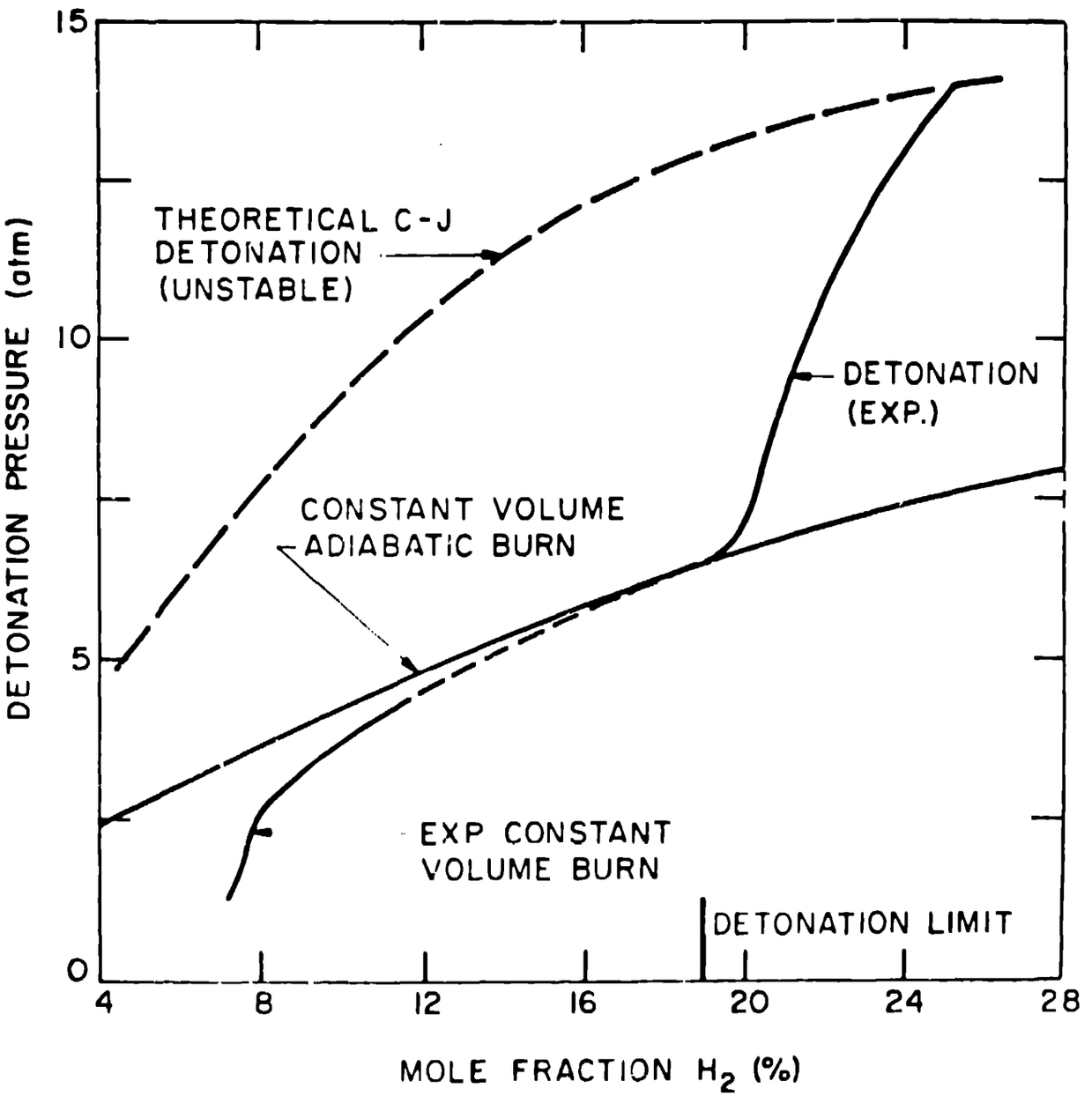
15
10
5
0
DETONATION PRESSURE (atm)
THEORETICAL C-J
DETONATION
(UNSTABLE)
DETONATION
(EXP.)
CONSTANT VOLUME
ADIABATIC BURN
EXP CONSTANT
VOLUME BURN
DETONATION LIMIT
4
8
12
16
20
24
28
MOLE FRACTION H_2 (%)

Fig. 2

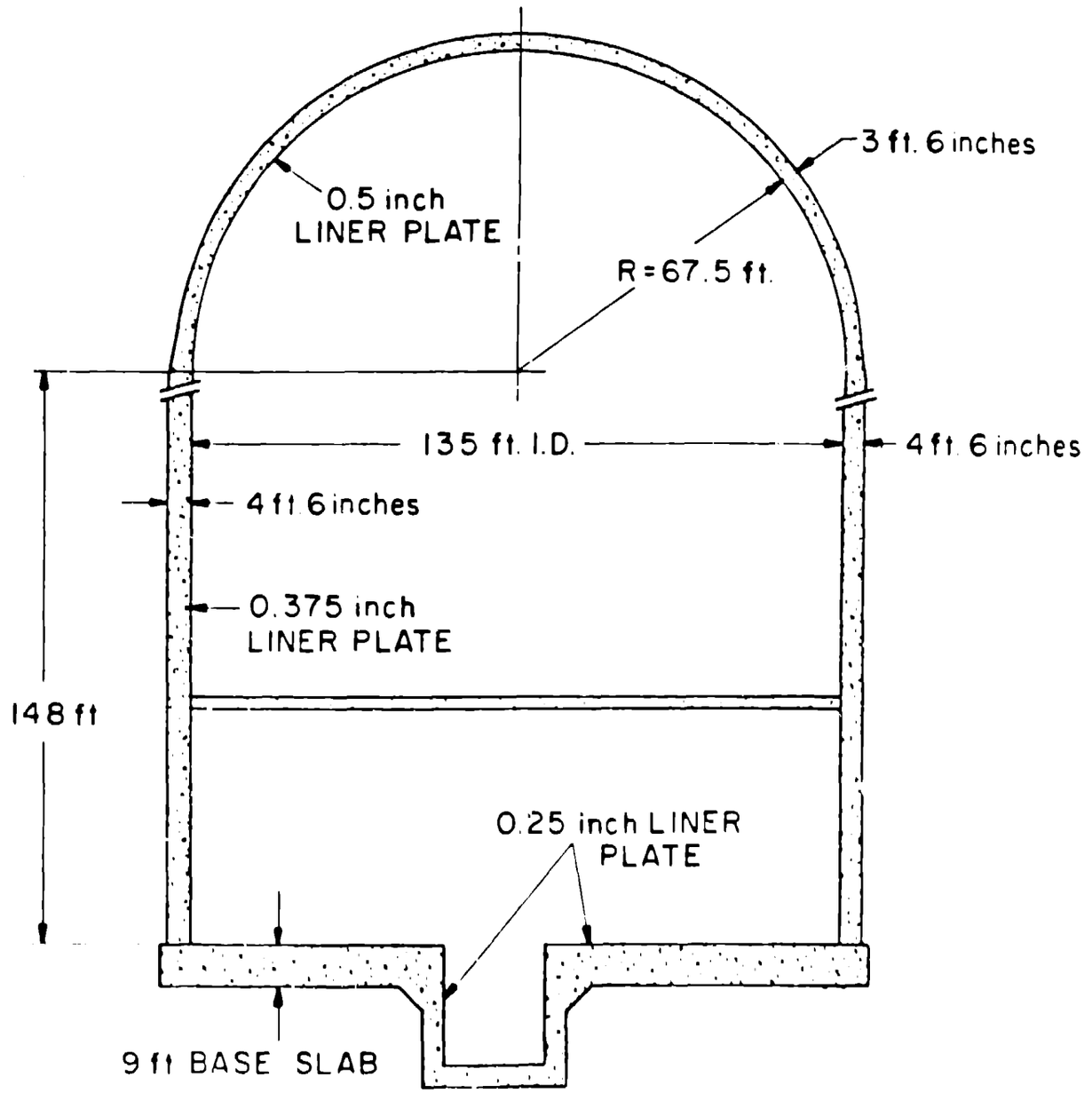
3 ft. 6 inches
0.5 inch
LINER PLATE
R = 67.5 ft.
135 ft. I.D.
4 ft. 6 inches
4 ft. 6 inches
0.375 inch
LINER PLATE
148 ft
0.25 inch LINER
PLATE
9 ft BASE SLAB

Fig. 3

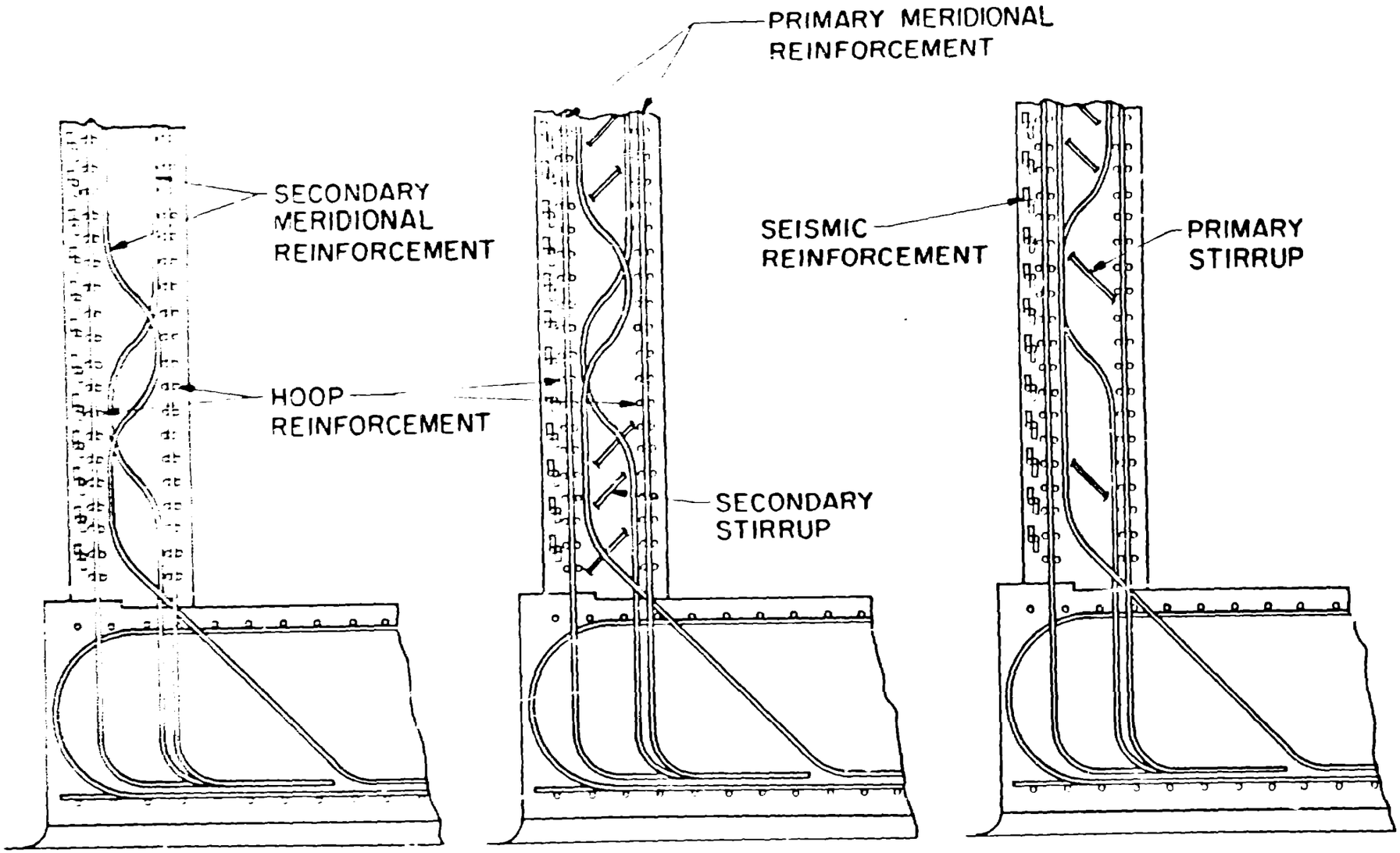
PRIMARY MERIDIONAL
REINFORCEMENT
SECONDARY
MERIDIONAL
REINFORCEMENT
HOOP
REINFORCEMENT
SECONDARY
STIRRUP
SEISMIC
REINFORCEMENT
PRIMARY
STIRRUP

Fig. 4

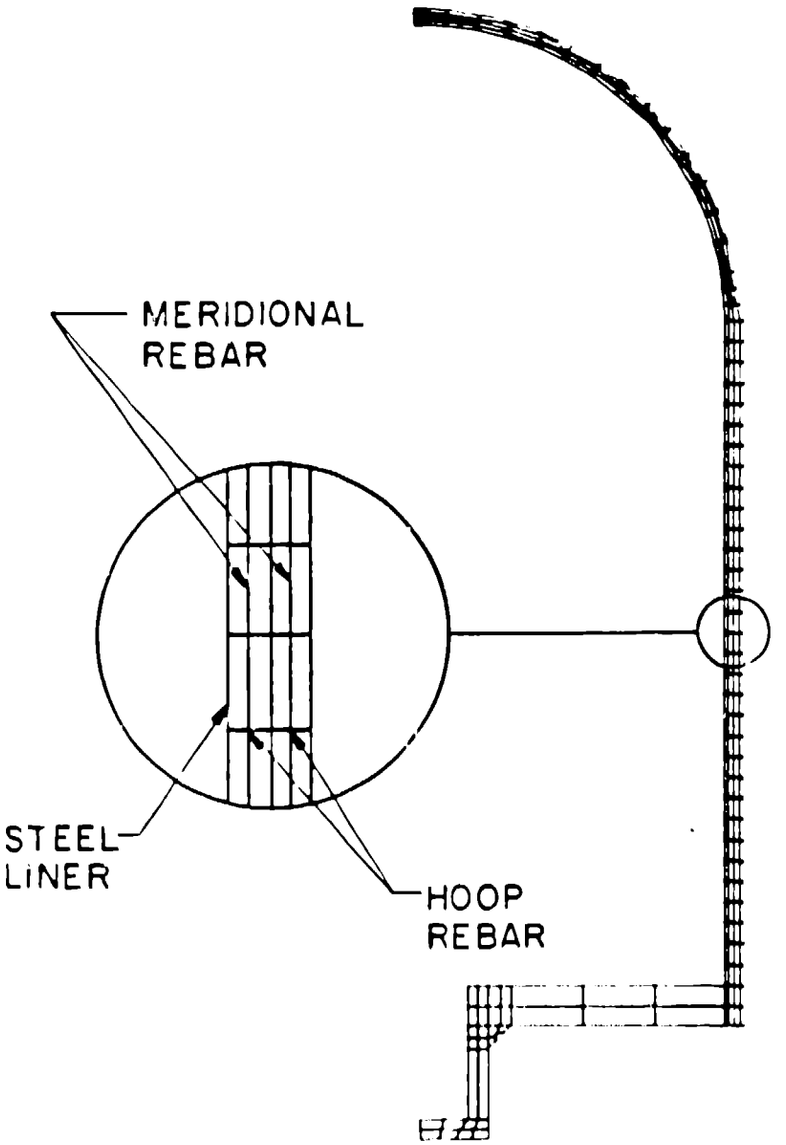

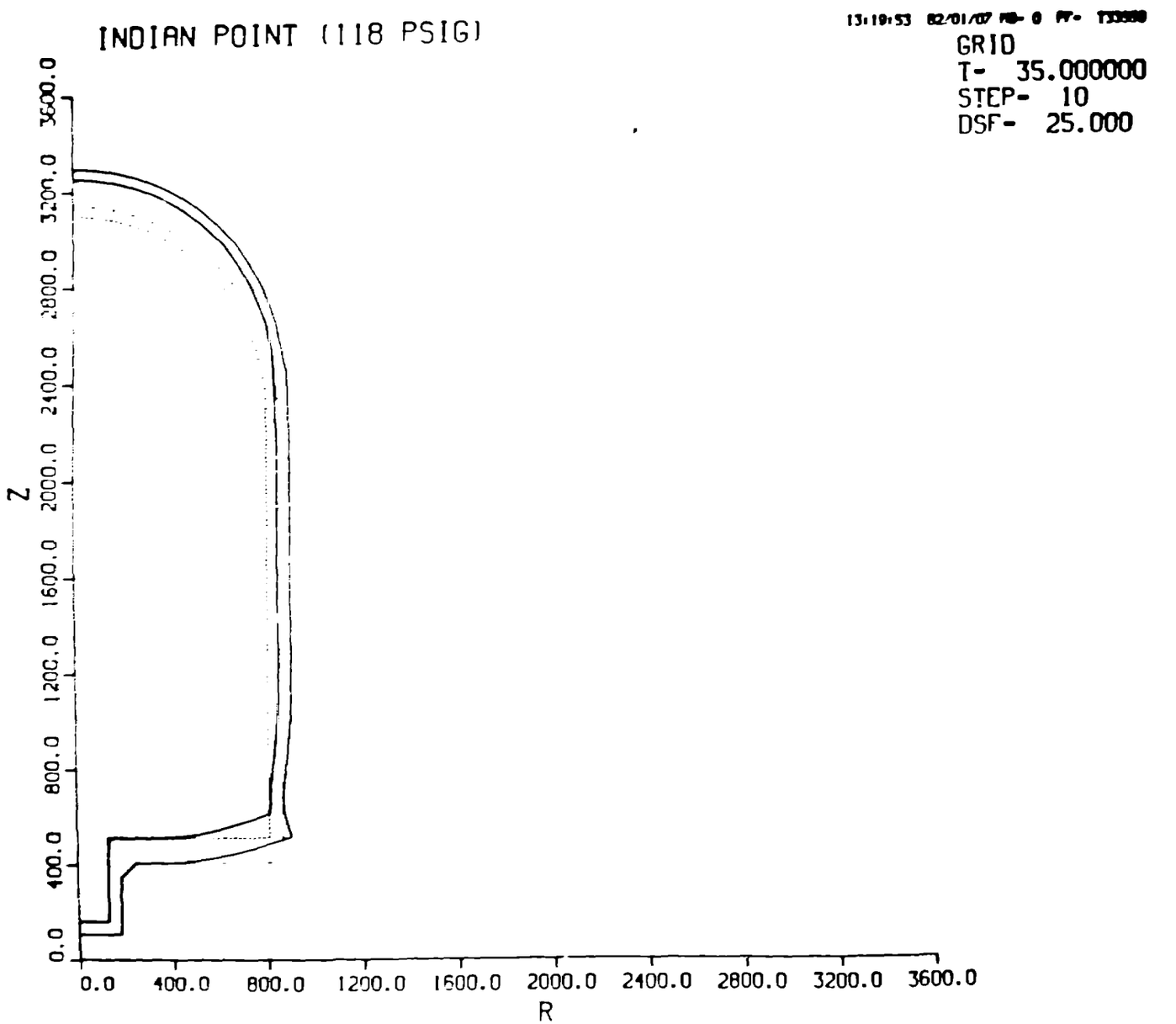
INDIAN POINT (118 PSIG)
13:19:53 82/01/07 PB- 0 PT- T33680
GRID
T- 35.000000
STEP- 10
DSF- 25.000
Z
0.0
400.0
800.0
1200.0
1600.0
2000.0
2400.0
2800.0
3200.0
3600.0
R
0.0
400.0
800.0
1200.0
1600.0
2000.0
2400.0
2800.0
3200.0
3600.0

Fig. 6

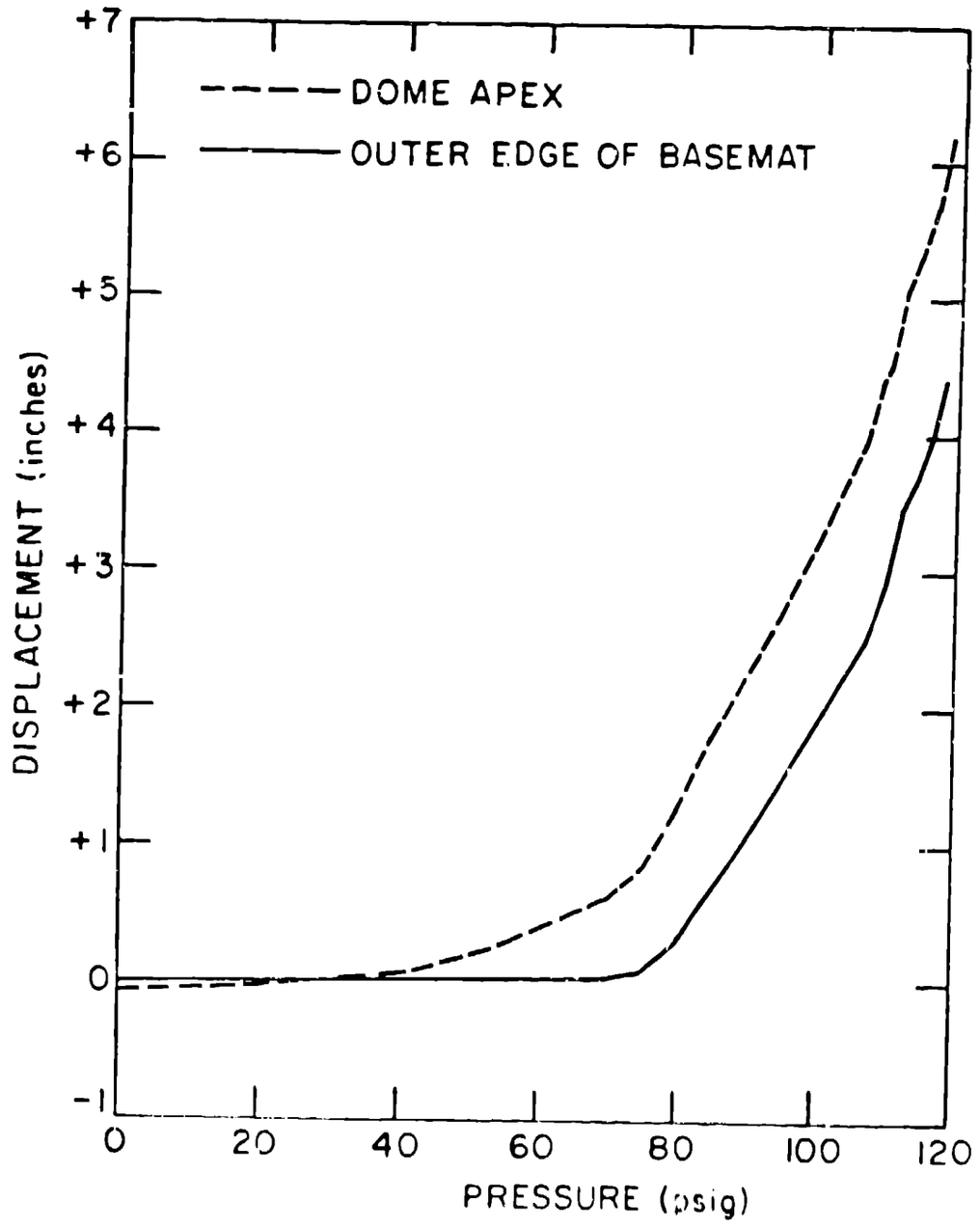
DOME APEX
OUTER EDGE OF BASEMAT
DISPLACEMENT (inches)
+7
+6
+5
+4
+3
+2
+1
0
-1
0
20
40
60
80
100
120
PRESSURE (psig)

Fig. 7

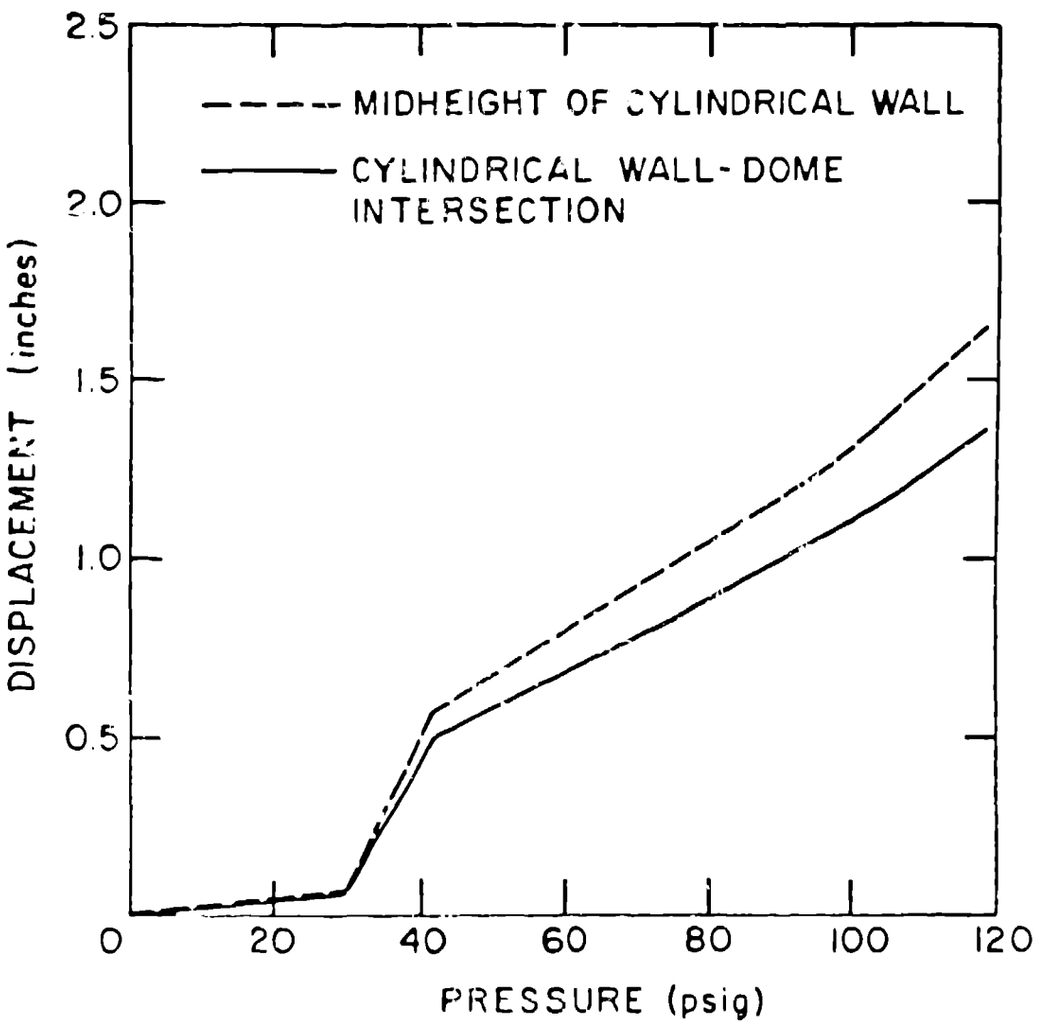
MIDHEIGHT OF CYLINDRICAL WALL
CYLINDRICAL WALL-DOME INTERSECTION
DISPLACEMENT (inches)
PRESSURE (psig)
2.5
2.0
1.5
1.0
0.5
0
20
40
60
80
100
120

Fig. 8

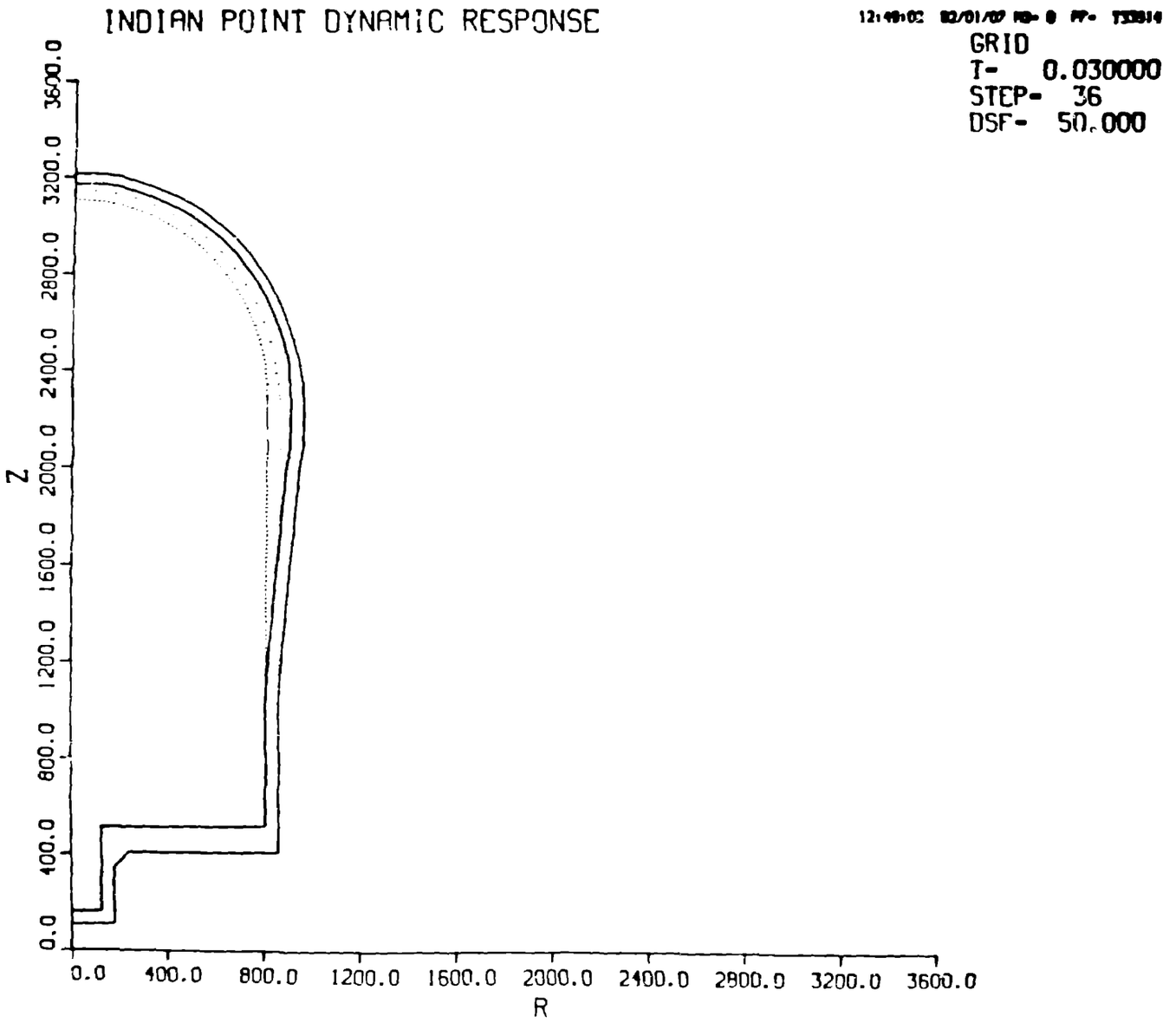
INDIAN POINT DYNAMIC RESPONSE
GRID
T- 0.030000
STEP- 36
DSF- 50.000
Z
R
0.0
400.0
800.0
1200.0
1600.0
2000.0
2400.0
2800.0
3200.0
3600.0

Fig. 9

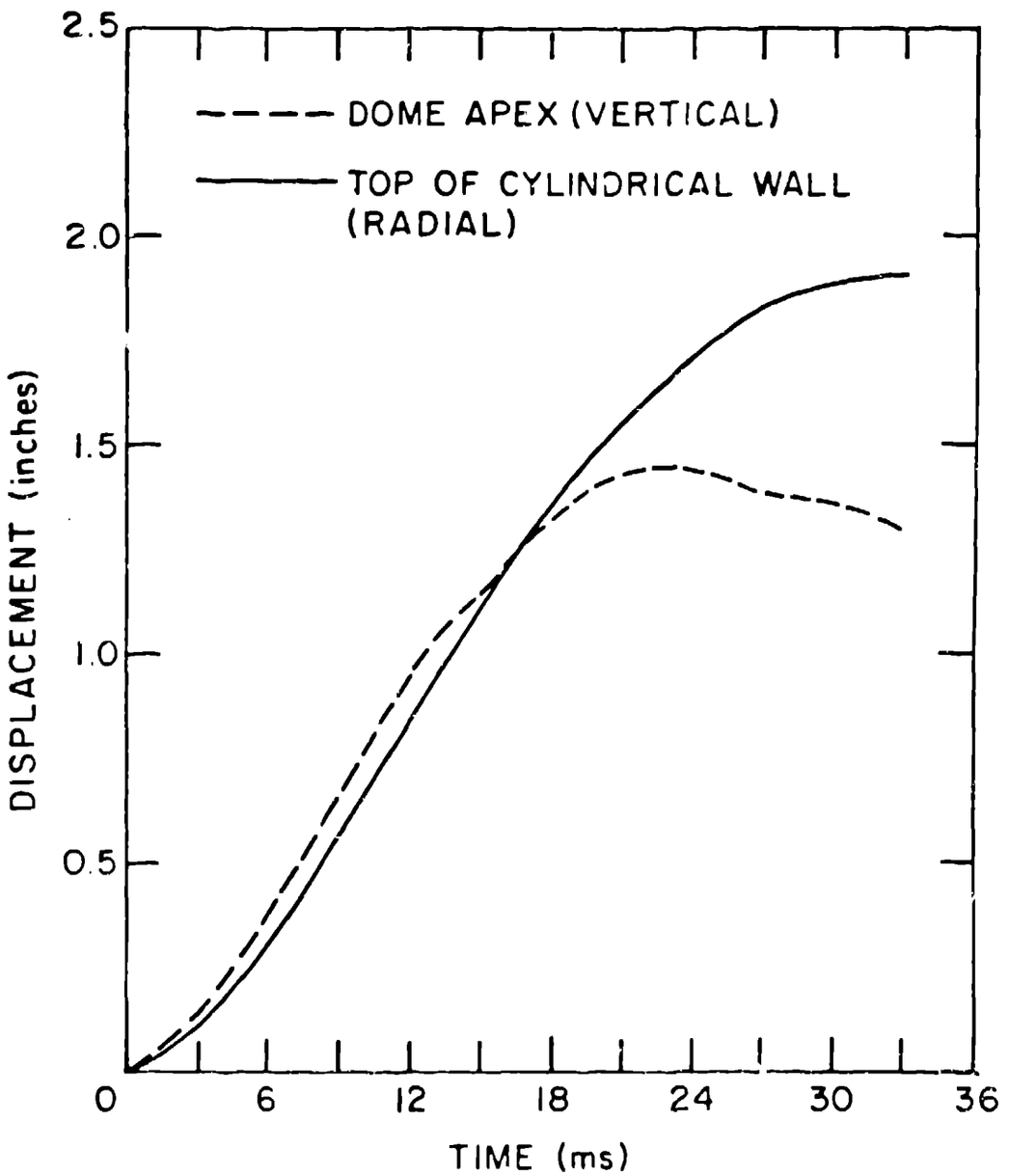
2.5
2.0
1.5
1.0
0.5
0
6
12
18
24
30
36
DOME APEX (VERTICAL)
TOP OF CYLINDRICAL WALL (RADIAL)
DISPLACEMENT (inches)
TIME (ms)